Proceedings of the Korean Nuclear Society Spring Meeting
Pohang, Korea, May 1999

Evaluation of Photonuclear Data of Mo, Zn, S and Cl for Medical Application

Young-Ouk Lee, Yinlu Han [1], Jeong-Yeon Lee and Jonghwa Chang
Korea Atomic Energy Research Institute
P.O Box 105 Yusung, Taejon, Korea

abstract

As part of IAEA CRP on "Compilation and evaluation of photonuclear application", we evaluated photoproduction data of Mo, Zn, S and Cl isotopes for medical use and biological application. Available experimental data were collected and their discrepancies were analyzed to select or reconstruct the representative data set. The photoabsorption cross sections were then evaluated by applying the Giant Dipole Resonance (GDR) model for the energies below about 30 MeV, and the quasi-deuteron model for energies below 140 MeV, which is the threshold for pion production. The resulting representative photoabsorption data were given as input for the theoretical calculations for the emission process of light nuclei including neutron, proton, deuteron, triton, He-3, alpha particles and gamma rays by use of the Hauser-Feschbach and the preequilibrium model. Appropriate optical model parameters were applied to prepare the transmission coefficients for the Hauser-Feshbach statistical model.

I. Introduction

Evaluated photonuclear data are important for a variety of applications such as radiation protection and dosimetry by accelerators in medical applications, calculations of absorbed dose in human body during radiotherapy and activation analyses using photonuclear reactions [1, 2]. The photonuclear reaction data have been widely used in basic scientific research on neutron binding energy, nuclear level structure and deformation. In response to growing needs for photonuclear data, the IAEA initiated a Coordinated Research Project (CRP) under the title "Compilation and evaluation of photonuclear application". As part of this project, we evaluated the photoproduction data of ^{99}Mo which is needed in ^{99}Tc production for medical use, and the photonuclear data of Mo, Zn,S and Cl isotopes for biological application.

Chapter II deals with the evaluations and analysis of experimental data. Chapter III describes theoretical models and evaluation techniques applied in the work. In chapter IV, evaluated cross sections are presented and compared with experimental data. Finally, we summarize this work in Chapter V.

II. Analysis of Experimental Data

1. ^{92,94,96,98,100}Mo

The natural Mo consists of seven isotopes, i.e. ^{92}Mo (14.84%), ^{94}Mo (9.25%), ^{95}Mo (15.92%), ^{96}Mo (16.68%), ^{97}Mo (9.55%), ^{98}Mo (24.13%) and ^{100}Mo (9.63%). The measured data of photoneutron cross sections for ^{92,94,96,98,100}Mo were first performed in 1974 by H. Beil, et al. [3] in the incident photon energy region from the threshold up to 30 MeV. The experimental data of

[1] Permanant Address: China Atomic Energy Research Institute

the (γ, n+np), (γ, 2n+2np), (γ, 3n), (γ, xn) reactions and total neutron production were given respectively. The quasi-monoenergetic photon beams were used in measuring photoneutron data. There are no experimental data reported up to now for ^{95,97}Mo.

2. ^{64,66,67,68,70}Zn

The natural Zn consists of five isotopes, i.e. ^{64}Zn (48.60%), ^{66}Zn (27.90%), ^{67}Zn (4.10%), ^{68}Zn (18.80%) and ^{70}Zn (0.60%). The measured data of photoneutron cross sections in the incident photon energy region from the threshold to 24 MeV were first performed by A.M. Goryachev, et al. [4] for ^{66,67,68,70}Zn in 1982. As for ^{64}Zn, most of the work of measuring photoneutron cross sections were carried out from 1951 to 1982. The experimental data of L. Katz, et al. [5], P. Carlos, et al. [6] and A.M. Goryachev, et al. basically agree according to the shapes, but there are differences in the magnitudes. The measured data of W.DEL. Bianco, et al. [7, 8] and G.E. Coote, et al. [9] are in agreement with Goryachev's data. Most of the measuring work used the same method, in which the photoneutron cross sections for reactions (γ, n) + (γ, np) and (γ, 2n) were measured with monochromatic photon beams in the energy range of 8 $\sim$ 30 MeV and a high efficiency neutron detecting system. Photoneutron yield curves were obtained for the isotopes ^{64,66,67,68,70}Zn, then the cross sections were calculated from the yields by means of the Penfold-Leiss method [4] with the step of 1.0 MeV in the Goryachev's work. The magnitude of Katz's data is quite different from others and there is no information on error analyses. In our evaluation, Katz's data were excluded and Goryachev's and Bianco's experimental data were used to guide theoretical calculation.

3. ^{32,34}S

The natural S consists of four isotopes, i.e. ^{32}S (95.02%), ^{33}S (0.75%), ^{34}S (4.21%) and ^{36}S (0.02%). In the present work, various available measured data of photonuclear reaction for S and its isotopes were collected from EXFOR master files and analyzed. There are two set of measured photonuclear reaction data for ^{32}S, which cover from the threshold to 32 MeV. The experimental data are from Saclay [10] and Canada [5] laboratories. Saclay laboratory gave the cross sections of the (γ, n + np), (γ, np), (γ, 2n) reactions and photoneutron productions, and performed an analysis of the competition among the (γ, n), (γ, np) and (γ, 2n) exit channels. Canada laboratory gave only ^{32}S(γ, np)^{30}P reaction cross sections. The cross sections for the γ + ^{34}S reaction were measured by Y.I. Assafiri, et al. [11] in 1984 and 1986, giving the photoabsorption cross section and (γ, n), (γ, p), (γ, 2n) and (γ, np) reaction cross sections from the threshold to 26 MeV. There are no experimental data reported up to now for the γ + ^{33,36}S reaction. The experimental data of Saclay laboratory and Y.I. Assafiri are used to guide theoretical calculation.

4. ^{35,37}Cl

The natural Cl consists of two isotopes, i.e. ^{35}Cl (75.77%) and ^{37}Cl (24.23%). The measurements of photoneutron cross sections for ^{nat}Cl were first performed by A. Veyssiere, et al. [10] for the incident photon energy region from the threshold to 28 MeV in 1974. The experimental data of the (γ, n+np), (γ, 2n+2np) reaction and total neutron production cross sections were given. The competition between the (γ, n), (γ, np) and (γ, 2n) exit channels was analysed. The experimental data were retrieved from EXFOR library and were used to guide adjusting model parameters.

III. Theoretical Models and Evaluation Techniques

There is no nuclear force and charge interaction between the photon and the nucleus, and thus the photonuclear reaction is induced by electromagnetic interaction. At low energies, below about 30 MeV, the Giant-Dipole Resonance (GDR) is the dominant excitation mechanism, where a collective bulk oscillation of the neutrons against the protons occurs. At higher energies below 140 MeV, the threshold for the pion production, where the wavelength of the photon decreases, the photoabsorption on a neutron-proton (quasi-deuteron: QD) which has a large dipole moment become important. Therefore, the photoabsorption cross section can be expressed as the sum of $\sigma_{\mathrm{GDR}}(\varepsilon_\gamma)$ and $\sigma_{\mathrm{QDM}}(\varepsilon_\gamma)$,

$$\sigma_{abs}(\varepsilon_\gamma) = \sigma_{\mathrm{GDR}}(\varepsilon_\gamma) + \sigma_{\mathrm{QDM}}(\varepsilon_\gamma). \tag{1}$$

In this work, photoabsorption cross sections in the GDR region were evaluated with GUNF code [12], in which E_1 and E_2 radiations are considered. The formulas of strength functions for E_1 and E_2 radiations used in the code are:

1. Lorenzian form with energy-dependent damping width for E_1 radiation [13]:

$$f_{E_1}(\varepsilon_\gamma) = K_{E_1} \sum_{i=1}^{n} \frac{\sigma_i \varepsilon_\gamma ,_i ,_i(\varepsilon_\gamma)}{(\varepsilon_\gamma^2 - E_i^2)^2 + \varepsilon_\gamma^2 ,_i^2(\varepsilon_\gamma)} \tag{2}$$

with

$$,_i(\varepsilon_\gamma) = ,_i \frac{\varepsilon_\gamma^2 + 4\pi^2 T^2}{E_i^2} \tag{3}$$

and

$$T^2 = \frac{B_n - \Delta - \varepsilon_\gamma}{a} \tag{4}$$

2. Lorenzian strength function for E_2 radiation:

$$f_{E_2}(\varepsilon_\gamma) = K_{E_2} \frac{\sigma \varepsilon_\gamma^{-1} ,^2}{(\varepsilon_\gamma^2 - E^2)^2 + \varepsilon_\gamma^2 ,^2} \tag{5}$$

The photonuclear absorption cross section is the sum of all the partial cross sections:

$$\sigma_{abs} = \sigma_{\gamma,n} + \sigma_{\gamma,p} + \sigma_{\gamma,d} + \sigma_{\gamma,t} + \sigma_{\gamma,He^3} + \sigma_{\gamma,\alpha} + \sigma_{\gamma,2n} + \ldots, \tag{6}$$

and photoneutron cross section is the sum of neutron producing cross sections as

$$\sigma_{\gamma,xn} = \sigma_{\gamma,n} + \sigma_{\gamma,np} + \sigma_{\gamma,2n} + \sigma_{\gamma,2np} + \sigma_{\gamma,3n} + \ldots \tag{7}$$

In the case of existence of the measured photoabsorption cross sections, the resonance parameters can be adjusted by fitting the available experimental data of photoabsorption cross sections. When there is no measured photoabsorption cross section, the photoneutron cross sections can be used to approximate the photoabsorption cross sections for heavy nuclei, since contributions from photoproton reactions and other reactions producing complex charged particles are suppressed by the Coulomb barrier. However, in light nuclei where the photoproton cross section is no longer small, the resonance parameters are adjusted in such a way that the decaying model calculation with the initial nuclear excitation reproduces available photonuclear reaction measurements. The GUNF code uses Hauser-Feshbach and exciton models for decaying model calculations to adjust the resonance parameters when only photoneutron measurements are given.

The QDM photoabsorption cross section $\sigma_{\rm QDM}(\varepsilon_\gamma)$ is expressed in terms of the quasi-deuteron model which uses a Levinger-type theory to relate the nuclear photoabsorption cross section to the experimental deuteron photodisintegration cross section $\sigma_d(\varepsilon_\gamma)$,

$$\sigma_{QDM}(\varepsilon_\gamma) = L\frac{NZ}{A}\sigma_d(\varepsilon_\gamma)f(\varepsilon_\gamma) \tag{8}$$

where the Levinger parameter was derived to be $L = 6.5$, and $f(\varepsilon_\gamma)$ is the Pauli-blocking function, which reduces the free deuteron cross section $\sigma_d(\varepsilon_\gamma)$ to account for Pauli-blocking of the excited neutron and proton by the nuclear medium. NZ is the total number of neutron-proton pairs inside the nucleus, and the free deuteron cross section is as follows:

$$\sigma_d(\varepsilon_\gamma) = 61.2\frac{(\varepsilon_\gamma - 2.224)^{\frac{3}{2}}}{\varepsilon_\gamma}\text{mb}. \tag{9}$$

The Pauli-blocking function was derived in the Ref. [14] to be a multidimensional integral whose solution could be well approximated in the energy range 20 to 140 MeV by a polynomical, as follows:

$$\begin{aligned} f(\varepsilon_\gamma) &= 8.3714 \times 10^{-2} - 9.8343 \times 10^{-3}\varepsilon_\gamma + 4.1222 \times 10^{-4}\varepsilon_\gamma^2 \\ &\quad -3.4762 \times 10^{-6}\varepsilon_\gamma^3 + 9.3537 \times 10^{-9}\varepsilon_\gamma^4 \end{aligned} \tag{10}$$

Since the Pauli-blocking function needs to be defined at all energies, the exponential shape was used for energies below 20 MeV and above 140 MeV, as follows:

$$f(\varepsilon_\gamma) = e^{-\frac{D}{\varepsilon}} \tag{11}$$

where D is a constant, 73.3 MeV for energy $\varepsilon_\gamma < 20$ MeV and 24.2 MeV for energy $\varepsilon_\gamma > 140$ MeV, respectively.

When the photoabsorption cross sections were established, the decaying processes including n, p, d, t and α particle emission up to 140 MeV were calculated using GNASH code [15]. The spherical optical model was used to calculate the transmission coefficients. The Hauser-Feshbach theory with full angular momentum and parity conservation calculated the equilibrium emission [16]. The preequilibrium theory was used to describe the processes of preequlibrium emission, and damping to equilibrium, during the evolution of the reaction. The theory for calculating photonuclear angular distributions, enabling a determination of the double differential cross sections of ejectiles and the multiple-preequilibrium emission processes which become important when the photon energy exceeds about 50 MeV were included in the calculation. The file of discrete level information and ground-state masses, spin and parities was provided, the mass values were based upon an interim set from Wapstra obtained prior to the 1988 publication, and supplemented in the case of unmeasured masses with values from the Moller and Nix calculations. The optical potential parameters were taken from Ref [17].

IV. Calculated Results

1. Resonance Parameters

The resonance parameters for $\gamma+^{92,94,96,98,100}$Mo were obtained based on the experimental data of photoneutron cross sections approximated as photoabsorption cross sections. We employed a Lorentzian strength function of single peak form, since Mo is a spherical nucleus. The resulting resonance parameters are given in Table 1.

For ^{64,66,67,68,70}Zn, the photoneutron cross sections can not be used to approximate the photoabsorption cross sections since the photoproton and the photoalpha cross sections are no longer small. The resonance parameters were adjusted to better reproduce the experimental data of photoneutron cross sections. We employed a Lorentzian strength function of double peak form since Zn is a deformed nucleus. The resulting resonance parameters are given in Table 2.

The resonance parameters for the $\gamma+^{32,34}$S reaction were obtained based on the experimental data of photoneutron cross sections with the same method as for the case of Zn isotopes. For the γ + ^{33,36}S reaction, the parameters of the ^{34}S were used, since there are no experimental data. We employed a Lorentzian strength function of double peak form, since S is a deformed nucleus. The resulting parameters are given in Table 3.

The resonance parameters for the $\gamma+^{35,37}$Cl reaction were obtained based on the experimental data of photoneutron cross sections for the γ + ^{nat}Cl reaction with the same method as for the case of Zn and S isotopes. We employed a Lorentzian strength function of double peak form, since Cl is a deformed nucleus. The resulting parameters are given in Table 4.

2. Photonuclear Cross Sections

In Fig. 1, the calculated results for the γ + ^{100}Mo reaction cross sections are compared with the experimental data taken from the Saclay laboratory [10]. The calculated results show that the overall shape and magnitude of photoneutron cross sections are in good agreement with the experimental data. There are slight discrepancies in some reaction channels between the model calculations and the experimental data which are mainly due to the separation of the total counts into (γ, n), (γ, 2n) and (γ, 3n) events in the experiments. ^{99}Mo, the medical radioisotope of interest, can be induced from the ^{100}Mo(γ, n)^{99}Mo reaction. The production cross sections for ^{99}Mo are also given in Fig. 1. The calculated results show that the production cross sections of ^{99}Mo increase sharply from incident photon energies of 8 MeV up to around 15 MeV, and decrease rapidly above 15 MeV.

The calculated results for ^{64,66,67,68,70}Zn(γ, n) reaction cross sections are compared with the experimental data in Fig. 2. The calculation photoneutron cross section agree well with the experimental data of Goryachev [4] and Bianco [8]. For the ^{64}Zn(γ, n+np) reaction, the calculated results are lower than the experimental data of Carlos [6] for incident photon energies E_γ >15 MeV, since the experimental data of Goryachev [4] were used to guide theoretical calculation. The photoneutron, photoproton, photoalpha cross sections and the particle production cross section are also given in Fig. 2 for the ^{64}Zn isotope. The results shows that the photoproton and the photoalpha cross sections are no longer small, and around 22 MeV the photoproton cross section exceeds the photoneutron cross section for the γ + ^{64}Zn reaction.

The comparision of calculated results with the experimental data for γ + ^{32}S reaction cross sections are given in Fig. 3. The calculated photoneutron cross sections and total neutron production cross sections agree with experimental data for the γ + ^{32}S reaction, and the calculated results of the ^{32}S(γ, 2n) reaction agree with the existing experimental data. For the ^{32}S(γ, np)^{30}P reaction, the theoretical results are in agreement with the experimental data of Saclay [10] for incident photon energies $E_\gamma < 26$ MeV. For energies $E_\gamma \geq 26$ MeV, the calculated results are higher than the experimental data of Saclay, but are lower than those of Katz [5]. This discrepancy between the calculated results and experimental data of Saclay [10] may be due the fact that the (γ, n) and (γ, np) reaction cross sections were separated from the photoneutron cross section in the experiment. The n, p, d, t and α emission cross sections as well as the production cross section for the γ + ^{32}S reaction were calculated up to 140 MeV, and are shown in Fig. 3.

The calculated results for γ + ^{35,37}Cl reaction cross sections are compared with the experimental data [10] in Fig. 4. Since the experimental data are natural nucleus ones, the calculated results for ^{35}Cl and ^{37}Cl were transformed into those for natural nucleus with the relation:

$$\sigma(^{nat}\mathrm{Cl}) = \sigma(^{35}\mathrm{Cl}) * 0.7577 + \sigma(^{37}\mathrm{Cl}) * 0.2423 \tag{12}$$

The calculated results are basically in agreement with experimental data for the (γ, n + np), (γ, 2n+2np) and (γ,n+np+2(2n+2np)) reactions. The calculated results for the photoabsorption, the particle emission and the particle production cross sections for energies up to 140 MeV are also given in Fig. 4.

V. Conclusion

As part of IAEA CRP on "Compilation and evaluation of photonuclear application", we evaluated the photoproduction data of Mo, Zn, S and Cl isotopes for medical use and biological application. Available experimental data were collected and their discrepancies were analyzed to select or reconstruct the representative data set. The photoabsorption cross sections were then evaluated by applying the Giant Dipole Resonance (GDR) model for the energies below about 30 MeV, and the quasi-deuteron model for energies below 140 MeV, which is the threshold for pion production. The resulting representative photoabsorption data were given as input for the theoretical calculations for the emission process of light nuclei, including neutron, proton, deuteron, triton, He-3, alpha particles and gamma rays by the use of the Hauser-Feschbach and the preequilibrium model. Appropriate optical model parameters were applied to prepare the transmission coefficients for the Hauser-Feshbach statistical model. The theoretical results are in good agreement with existing experimental data. Therefore, the calculated data are reliable and are recommended for incident photon energy $E_\gamma \leq 140$MeV.

Acknowledgements

This work was performed under the auspices of Korea Ministry of Science and Technology as one of the long-term nuclear R&D programs, and by IAEA Contract No.10547/R0. One of the authors (Y. Han) is grateful to the Korea Science and Engineering Foundation for giving him an opportunity to carry out this work under the Brain Pool program.

References

[1] Lee, Y., *et al.*: Evaluation of Photoneutron Cross Sections for Ta-181 in Giant Resonance Region. In *Korean Physics Society Fall Conference, Oct. 17-18, Kwang-Un Univ.* (1997).

[2] Lee, Y. *et al.*: Evaluation of Photonuclear Reaction Data on Tantalum-181 up to 140 MeV. *J. of Nucl. Sci. and Tech.*, **350**, 685 (1998).

[3] Beil, H. *et al.*: A Study of the Photoneutron Contribution to the Giant Dipole Resonance in Doubly Even Mo Isotopes. *Nucl. Phys.*, **A219**, 61,427 (1974).

[4] Goryachev, A. *et al.*: The Studying of the Photoneutron Reactions Cross Sections in the Region of the Giant Dipole Resonanse in Zinc, Germanium, Selenium, and Strontium Isotopes. *Voprosy Teoreticheskoj Yadernoj Fiziki*, **8**, 121 (1982).

[5] Katz, L. *et al.*: The Solution of X-Ray Activation Curves for Photonuclear Cross Sections. *J. Canada Phys.*, **29**, 518 (1951).

[6] Carlos, P. *et al.*: A study of the Photoneutron Contribution to the Giant Dipole Resonance of Nuclei in the A = 64 - 86 Mass Region. *Nucl. Phys.*, **A258**, 365 (1976).

[7] Bianco, W. *et al.*: Photonuclear Activation by 20.5-MeV Gamma Rays. *Phys. Rev.*, **126**, 709 (1962).

[8] Bianco, W. *et al.*: ^{64}Zn(γ,,n)^{63}Zn Cross Section from 20.4 to 21.9 MeV. *J. Canada Phys.*, **51**, 1302 (1973).

[9] Coote, G. *et al.*: Cross Sections for the (γ,n) Reaction in ^{63}Cu, ^{65}Cu, ^{64}Zn, ^{121}Sb, and ^{141}Pr, Measured with Monochromatic gamma rays. *Nucl. Phys.*, **23**, 468 (1961).

[10] Veyssiere, A. *et al.*: A Study of the Photoneutron Contribution to the Giant Dipole Resonance of s-d Shell Nuclei. *Nucl. Phys.*, **A227**, 513 (1974).

[11] Y.I, A. *et al.*: Photoneutron Cross Section of ^{34}S. *Nucl. Phys.*, **A413**, 416 (1984).

[12] Zhang, J.: Illustration of Photonuclear Data Calc. with GUNF Code. *Commu. of Nucl. Data Prog.*, **19**, 33 (1998).

[13] Kopecky, J. *et al.*: Test of Gamma-Ray Strength Functions in Nuclear-Reaction Model-Calculations. *Phys. Rev. C*, **41**, 1941 (1990).

[14] Chadwick, M. *et al.*: Pauli-blocking in the Quasideuteron Model of Photoabsorption. *Phys. Rev. C*, **44**, 814 (1991).

[15] Chadwick, M. *et al.*: Photonuclear Reactions in the GNASH code. Technical Report UCRL-ID-118721, Lawrence Livermore National Laboratory, Livermore, CA (1994).

[16] Chadwick, M. B., *et al.*: Photonuclear angular distribution systematics in the quasideuteron regime. *Journal of Nuclear Science and Technology*, **32**, 1154 (1995).

[17] Perey, C. M. *et al.*: Compilation of Phenomenological Optical Model Parameters. *Atomic Data and Nucl. Data Tables*, **17**, 1 (1976).

Table 1: The giant resonance parameters for $\gamma+^{92,94,96,98,100}$Mo reaction

	$\sigma_1^{E_1}$(b)	$,_1^{E_1}$(MeV)	$E_1^{E_1}$(MeV)	σ^{E_2}(b)	$,^{E_2}$(MeV)	E^{E_2}(MeV)
^{92}Mo	0.1624	5.9549	17.1062	0.9763	2.6526	15.5828
^{94}Mo	0.1680	6.0470	16.7468	0.2583	3.7496	13.4483
^{96}Mo	0.1516	8.0378	16.4252	0.1286	3.8950	17.3841
^{98}Mo	0.1096	12.3926	16.3712	0.4096	3.4531	16.1338
^{100}Mo	0.1220	10.0328	15.7193	0.2940	4.0740	16.8616

Table 2: The resonance parameters for $\gamma+^{64,66,67,68,70}$Zn reaction

	$\sigma_1^{E_1}$(b)	$,_1^{E_1}$(MeV)	$E_1^{E_1}$(MeV)	$\sigma_2^{E_1}$(b)	$,_2^{E_1}$(MeV)	$E_2^{E_1}$(MeV)	σ^{E_2}(b)	$,^{E_2}$(MeV)	E^{E_2}(MeV)
^{64}Zn	0.0382	5.9552	16.3200	0.0477	7.8976	18.2847	0.1524	4.7099	21.7498
^{66}Zn	0.0586	5.9449	16.2109	0.0248	7.7390	18.4633	0.1853	4.8776	21.6431
^{67}Zn	0.0750	9.6205	17.2285	0.0718	5.8581	20.9690	0.3122	3.1147	22.7351
^{68}Zn	0.0646	6.7963	16.1555	0.0374	5.4276	19.3646	0.3590	3.9957	21.9154
^{70}Zn	0.0544	9.9647	16.7183	0.1392	6.2289	19.8332	0.3595	2.4302	22.6181

Table 3: The resonance parameters for $\gamma+^{32,34}$S reaction

	$\sigma_1^{E_1}$(b)	$,_1^{E_1}$(MeV)	$E_1^{E_1}$(MeV)	$\sigma_2^{E_1}$(b)	$,_2^{E_1}$(MeV)	$E_2^{E_1}$(MeV)
^{32}S	0.03705	8.596995	20.19130	0.00335	10.324014	27.27399
^{33}S	0.02800	6.102877	17.29532	0.04200	4.6280310	22.05062
^{34}S	0.02800	6.102877	17.29532	0.04200	4.6280310	22.05062
^{36}S	0.02800	6.102877	17.29532	0.04200	4.6280310	22.05062

Table 4: The resonance parameters for $\gamma+^{35,37}$Cl reaction

	$\sigma_1^{E_1}$(b)	$,_1^{E_1}$(MeV)	$E_1^{E_1}$(MeV)	$\sigma_2^{E_1}$(b)	$,_2^{E_1}$(MeV)	$E_2^{E_1}$(MeV)
^{35}Cl	0.0406	8.965374	18.280561	0.0162	8.203328	21.148212
^{37}Cl	0.0177	11.92355	19.891900	0.0243	9.731074	23.89612

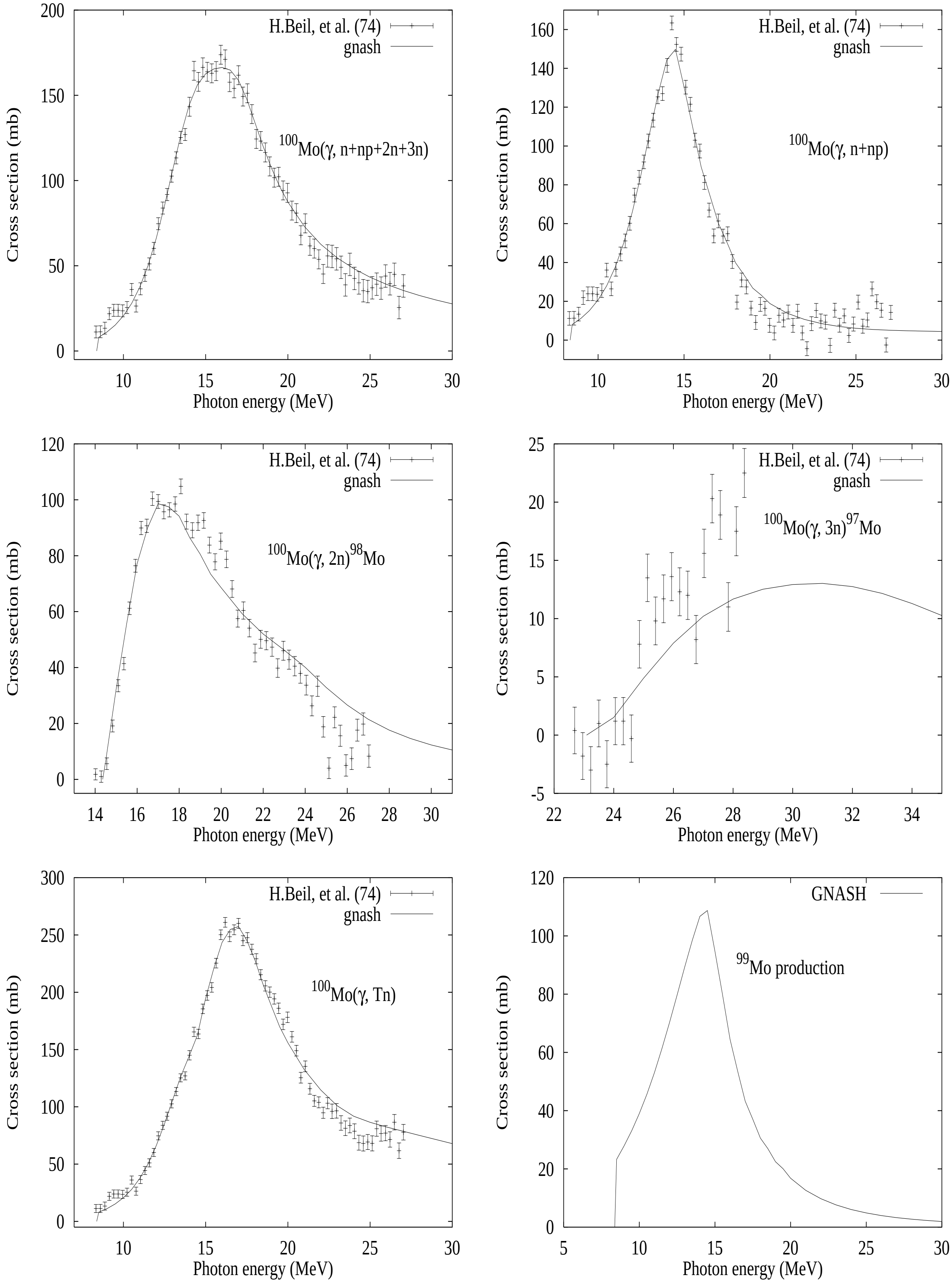

Figure 1: The comparison of calculated results with experimental data for ^{100}Mo photonuclear reaction cross sections

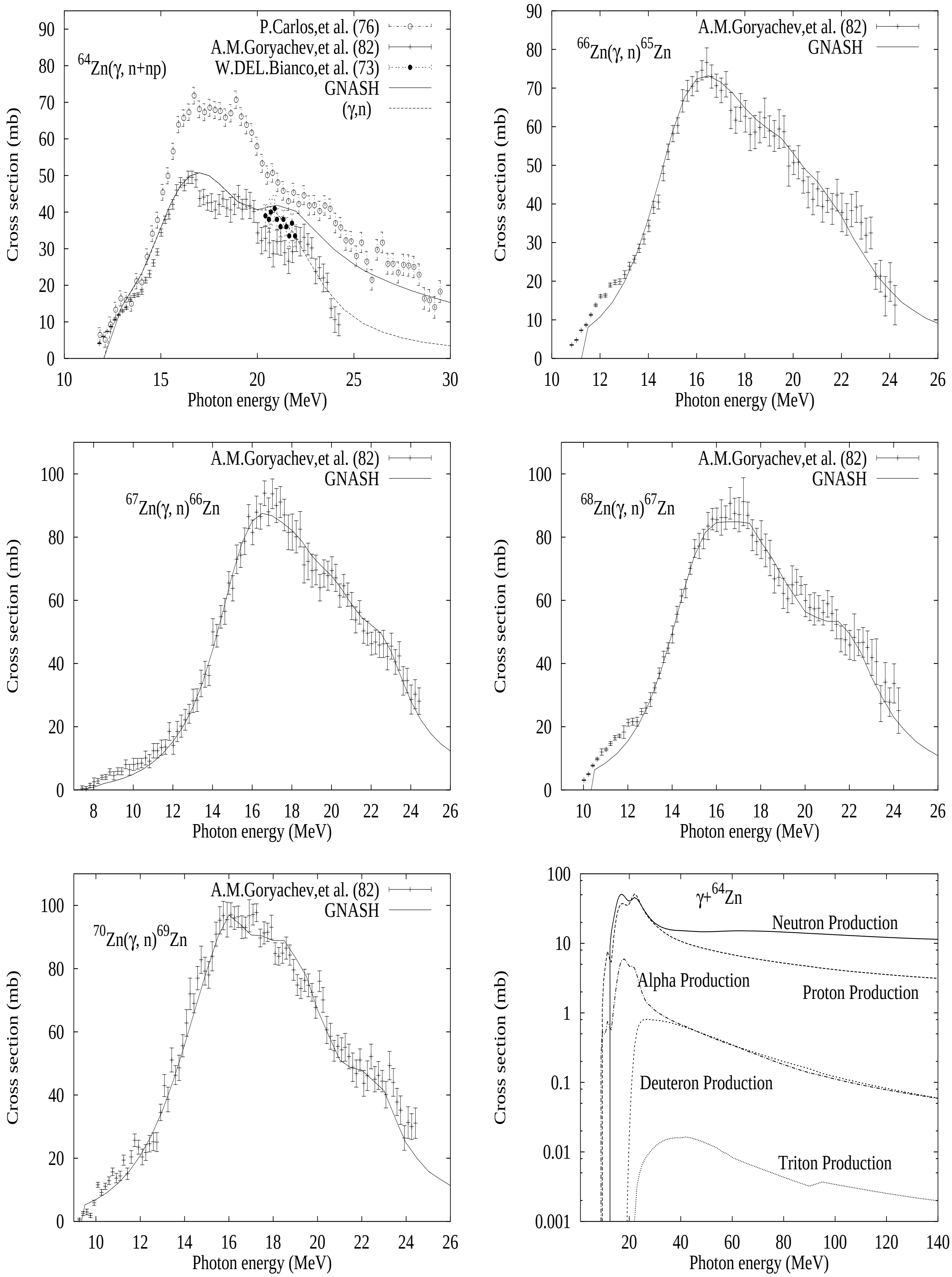

Figure 2: The comparison of calculated results with experimental data for ^{64,66,67,68,70}Zn photonuclear reaction cross sections

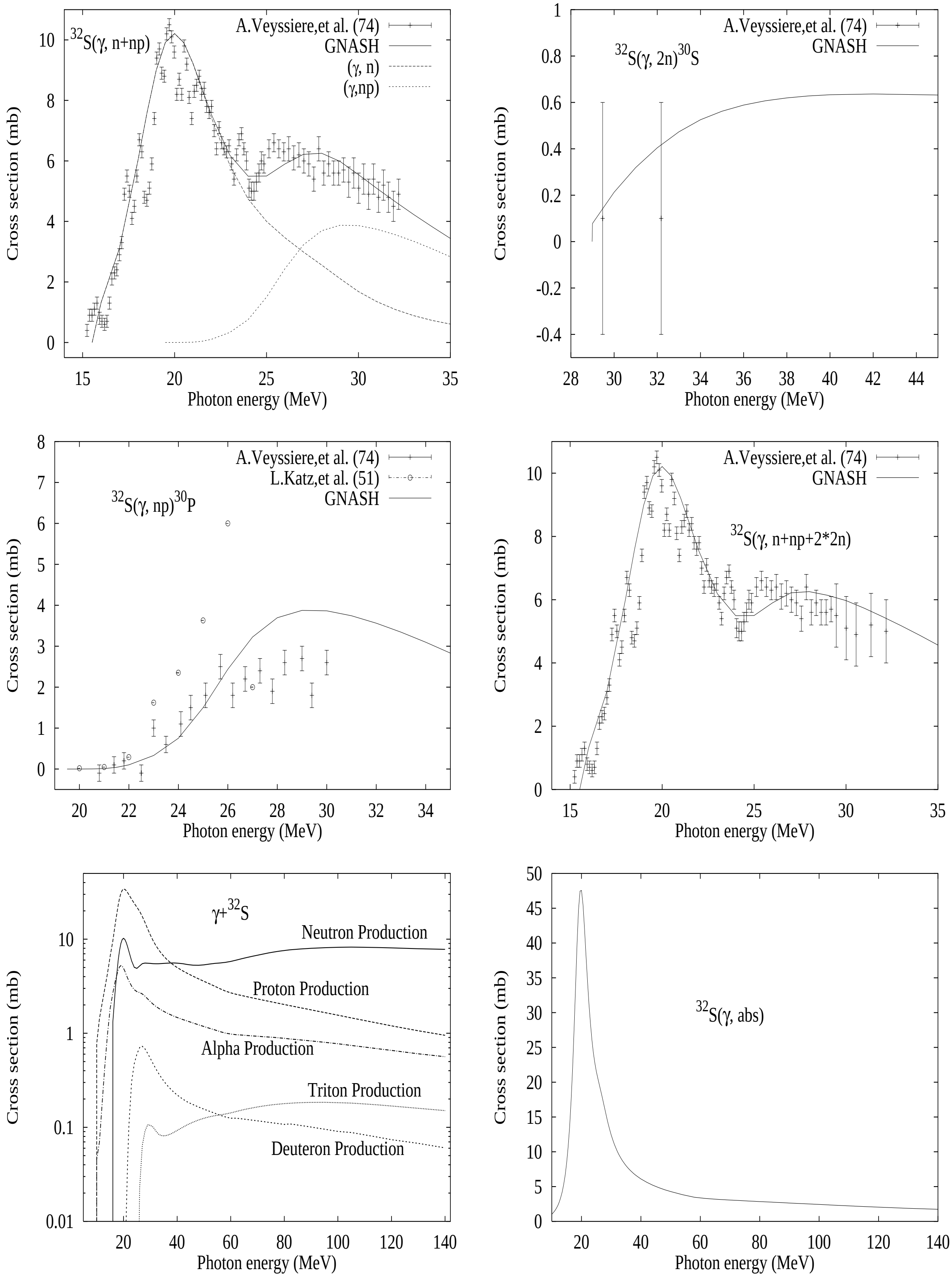

Figure 3: The comparison of calculated results with experimental data for ^{32}S photonuclear reaction cross sections

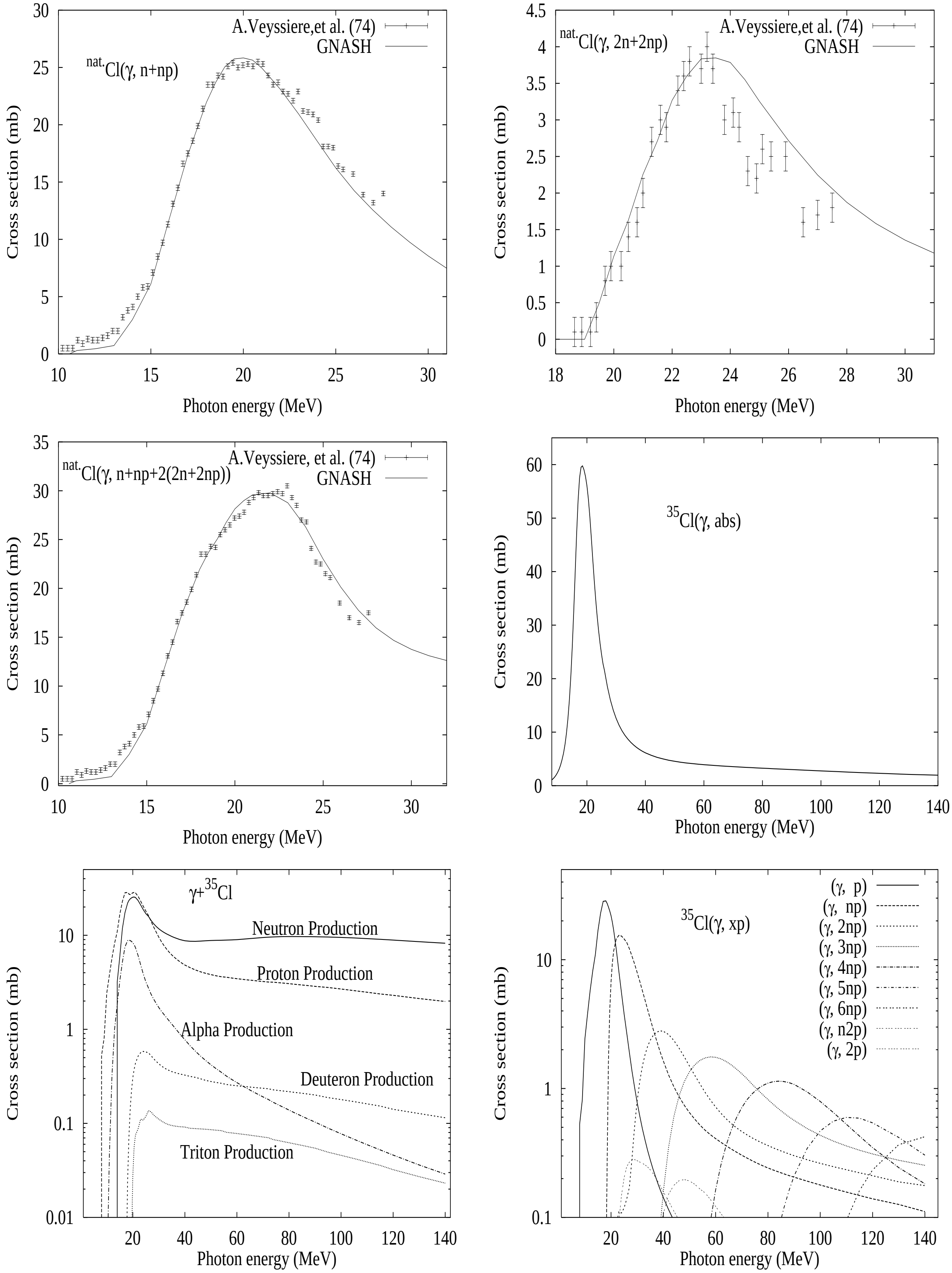

Figure 4: The comparison of calculated results with experimental data for ^{35,37}Cl photonuclear reaction cross sections